

# Wavelet-Aggregated Signal and Synchronous Peaked Fluctuations in Problems of Geophysical Monitoring and Earthquake Prediction

A. A. Lyubushin, Jr.

Schmidt United Institute of Physics of the Earth, Russian Academy of Sciences,  
Bol'shaya Gruzinskaya ul. 10, Moscow, 123810 Russia

Received June 5, 1999

**Abstract**—An algorithm for the construction of an aggregated signal of geophysical monitoring systems from multivariate time series is described. This algorithm uses wavelets as a basis functions, which allows the detection of common signals, including short-range earthquake precursors, that are unrecognizable by spectral methods. The effectiveness of the technique proposed is exemplified by the detection of short-term precursors to the Tien Shan, China earthquake of July 28, 1976, from the combined observation of ten geophysical parameters.

## INTRODUCTION

This paper addresses the analysis of multidimensional time series of geophysical monitoring systems recording synchronous variations in different geophysical fields at network stations. The so-called "low-frequency background processes" in the crust, such as variations in the groundwater level, deformations, tilts, electrical resistivity of rocks, concentration of chemical elements in groundwater, and so on, are the main object of this study.

In order to analyze such multidimensional time series, Lyubushin [1993, 1994, 1998a] developed methods for detecting a synchronization signal in variations of different geophysical fields (with the determination of synchronization frequency bands and time intervals). These methods, using the moving time-window technique, estimate the evolution of spectral matrix eigenvalues and canonical coherences, and synchronization is recognized as a peak in these statistics. The identification of such signals is based on the most general regularities in the behavior of complex systems, as they approach a catastrophe or a phase transition; these regularities are an increase in the spatial radius of fluctuations ("critical opalescence") and magnification of the collective component in the behavior of different parts of a complex system [Gilmore, 1984; Nikolis and Prigogine, 1990]). This approach was used in the search for strong-earthquake precursors in Kamchatka from geochemical data [Lyubushin, *et al.*, 1997, Lyubushin, 1998a].

Lyubushin, [1998b] proposed the construction of an aggregated signal, which is a scalar signal providing maximum information on the most general variations common to all processes analyzed and suppressing components typical of an individual process; the latter are commonly local disturbances caused by station site

conditions, anthropogenic factors, or measurement errors. As distinct from frequency-time diagrams, the aggregated signal often gives a geophysically clearer representation (in the form of a plot of one signal) demonstrating the behavior of the most general components present in all of the measured values, which makes the use of the accumulated experience and intuition more effective.

All the methods mentioned above are based on the spectral approach; i.e., they use, in one way or the other, harmonic expansions (even if nonparametric methods of the vector autoregression were employed). This has its pros and cons: these methods are best suited to the detection of common harmonic components, but they are however incapable of identifying strongly nonstationary (transient) common signals. Application of the moving time window technique is the only means for estimating the signal nonstationarity by using spectral methods. However, such a procedure averages transient signals, and their time characteristics are determined to within the length of the time window. On the other hand, the use of overly short windows makes spectral estimates unstable and enhances the effect of noise components.

Nearly all models of the earthquake preparation are known to indicate magnification of the collective component in the behavior of geophysical fields in the preparation zone as the moment of earthquake occurrence is approached [Kasahara, 1981; Sobolev, 1993]. Long- and middle-term precursors are smooth common variations in the behavior of geophysical fields and, consequently, one may hope to detect them by spectral methods; on the other hand, short-term precursors are generally impulsive, transient variations (e.g., due to the breakup of bridges between fractures in a source), and spectral methods fail to reveal them against the background of an intense noise.

The solution to this problem is provided by the wavelet theory, which originated in the mid-1980s. Elaborating this theory in the late 1980s, the French mathematician Ingrid Daubechies constructed a strict mathematical theory of signal expansions in orthogonal functions with a finite support (i.e., in wavelets) and formulated the concept of multiresolution analysis. Since then, the wavelets have been widely applied to the theory of signals, approximation of functions, data compression, and computer graphics.

In this paper, an algorithm is proposed for the construction of an aggregated signal of multivariate time series of low-frequency geophysical monitoring systems; the algorithm is conceptually identical to that described by Lyubushin [1998b], but uses wavelets as basis functions, rather than complex oscillating exponents. This allows the recognition of common signals undetectable by spectral methods (in particular, short-term earthquake precursors). The efficiency of the proposed technique is exemplified by the detection of short-term precursors to the Tien Shan, China earthquake of July 28, 1976.

CONSTRUCTION OF A WAVELET-AGGREGATED SIGNAL

Let  $x(t)$  be a function (signal) of a continuous real argument  $t$  (time) belonging to the space  $L_2(-\infty, +\infty)$  of functions square integrable over the entire real axis. Orthogonal multiresolution analysis (MRA) of a function  $x(t)$  is defined by the formula [Daubechies, 1988, 1992]

$$x(t) = \sum_{\alpha=-\infty}^{+\infty} x^{(\alpha)}(t), \tag{1}$$

$$x^{(\alpha)}(t) = \sum_{j=-\infty}^{+\infty} c^{(\alpha)}(\tau_j^{(\alpha)})\psi^{(\alpha)}(t-\tau_j^{(\alpha)}), \tau_j^{(\alpha)} = j \times 2^\alpha.$$

Here,  $\alpha$  is the number of a detail level, and

$$c^{(\alpha)}(\tau_j^{(\alpha)}) = \int_{-\infty}^{+\infty} x(t)\psi^{(\alpha)}(t-\tau_j^{(\alpha)})dt$$

are wavelet-coefficients at an  $\alpha$ th detail level corresponding to a time moment  $\tau_j^{(\alpha)}$ ;  $\psi^{(\alpha)}(t)$  are  $\alpha$ th level basis functions obtained from the mother wavelet  $\Psi(t)$  by its extensions and translation:

$$\begin{aligned} \psi^{(\alpha)}(t) &= (\sqrt{2})^{-\alpha}\Psi(2^{-\alpha}t), \\ \psi^{(\alpha)}(t-\tau_j^{(\alpha)}) &= (\sqrt{2})^{-\alpha}\Psi(2^{-\alpha}t-j). \end{aligned} \tag{2}$$

The construction of  $\Psi(t)$  is the main mathematical difficulty in obtaining the MRA -expansion. This function should be finite (in contrast to the classic Fourier analysis, where basis functions (sines and cosines) have an infinite support) and has the unit norm in  $L_2(-\infty, +\infty)$ ;

moreover, the infinite set of functions  $\{\psi^{(\alpha)}(t-\tau_j^{(\alpha)})\}$ , which are copies of the mother wavelet shifted to points  $\tau_j^{(\alpha)}$  and stretched by a factor of  $2^\alpha$ , should form an orthonormal basis in  $L_2(-\infty, +\infty)$ . For example, if

$$\begin{aligned} \Psi(t) &= -1 \text{ for } t \in \left(0, \frac{1}{2}\right], \\ &+1 \text{ for } t \in \left(\frac{1}{2}, 1\right], \text{ and } 0 \text{ for other } t, \end{aligned} \tag{3}$$

formula (1) corresponds to the MRA expansion of the function  $x(t)$  in the Haar wavelets. Most widespread is the family of the Daubechies mother wavelet functions  $\Psi(t) = D_{2p}(t)$  of an order  $2p$ , such that [Daubechies, 1988, 1982; Chui, 1992]

$$\begin{aligned} D_{2p}(t) &= 0 \text{ outside the interval } [-p+1, p], \\ \int_{-\infty}^{+\infty} t^k D_{2p}(t)dt &= 0 \text{ for } k = 0, 1, \dots, (p-1). \end{aligned} \tag{4}$$

Note that the Haar wavelet (3) is the Daubechies wavelet of the second order ( $p = 1$ ).

Wavelet-functions of greater orders are smoother and, consequently, more appropriate for the analysis of smooth functions. The Haar wavelet is suitable for detecting stepped components of a signal. At greater detail level indexes  $\alpha$ , the coefficients  $c^{(\alpha)}(\tau_j^{(\alpha)})$  account for larger-scale (“low-frequency”) variations in the signal  $x(t)$  in the vicinity of the points  $\tau_j^{(\alpha)}$  at a coarser mesh of their values.

Now, I consider a more realistic situation when  $x(t)$  is a signal with a discrete time  $t$  corresponding to  $N$  samples:  $t = t_j = j\Delta t, j = 1, \dots, N$ . To facilitate the subsequent use of the fast wavelet-transform [Daubechies, 1988, 1992; Chui, 1992; Press *et al.*, 1996],  $N$  is set equal to an integer of the form  $2^m$ . If  $N$  is unequal to  $2^m$ , where  $m$  is the least integer for which  $N \leq 2^m$ , the signal is complemented by zeros until its length becomes equal to  $2^m$  (this situation is completely analogous to the use of the fast Fourier transform).

In the case of a finite sample and discrete time, the MRA expansion is defined by the formula

$$\begin{aligned} x(t) &= d + \sum_{\alpha=1}^m x^{(\alpha)}(t), \\ x^{(\alpha)}(t) &= \sum_{j=1}^{2^{(m-\alpha)}} c^{(\alpha)}(\tau_j^{(\alpha)})\psi^{(\alpha)}(t-\tau_j^{(\alpha)}), \\ \tau_j^{(\alpha)} &= j \times 2^\alpha \Delta t. \end{aligned} \tag{5}$$

Therefore, in the discrete case, the first detail level has the smallest scale, and the total number of detail levels  $m$  depends on the sample length. The coefficient

$d$  in (5) is equal to the average of the numbers  $x(t)$ ,  $t = 1, \dots, N$ . The values of  $c^{(\alpha)}(\tau_j^{(\alpha)})$  and  $d$  are calculated by means of the forward fast wavelet transformation involving  $O(N)$  operations, whereas the fast Fourier transformation requires a greater number of operations  $O(N \log(N))$ . They uniquely determine the original sample  $x(t)$ , which can be recovered from given  $c^{(\alpha)}(\tau_j^{(\alpha)})$  and  $d$  by means of the inverse fast wavelet transformation. For the sake of simplicity and without loss of generality, I assume hereinafter that  $\Delta t = 1$ , i.e. the time will be measured in the units of the sampling interval.

The detail level can be associated with the frequency number (a frequency discrete) in the classical discrete Fourier transformation. A distinctive feature of the MRA expansion consists in the fact that the set of wavelet frequencies is considerably sparser (being uniform on a logarithmic scale) than in the Fourier analysis. This is what we pay for such a very important feature as the finiteness of basis functions, which is lacking in Fourier expansions and which enables a much more accurate localization of short-lived (transient) anomalies. Moreover, the finiteness of basis functions allows one to apply the wavelet analysis to nonstationary and non-Gaussian time series, the Fourier analysis of which is formally possible but ineffective.

Let  $q$  time series  $V^{(k)}(t)$ ,  $t = 1, \dots, N$ ;  $k = 1, \dots, q$ ;  $q > 2$  represent synchronous records of physical fields that are similar or differ in their nature, measured at different observation points of a monitoring network.

First of all, because series of low-frequency geophysical monitoring commonly incorporate the major portion of low-frequency variations, I will consider an incremental series, retaining the same notation as for the initial series.

Furthermore, I introduce a moving time window of adaptation  $r$  samples wide and normalize the time series to a uniform range of values, which is necessary for the combined analysis of heterogeneous time series, involving different scales:

$$U^{(k)}(t) := V^{(k)}(t) / (V_{\max}^{(k)}(1, r) - V_{\min}^{(k)}(1, r)) \quad (6a)$$

at  $1 \leq t \leq (r + 1)$

$$U^{(k)}(s + r) := V^{(k)}(s + r) / (V_{\max}^{(k)}(s, r) - V_{\min}^{(k)}(s, r)) \quad (6b)$$

at  $s > 1$

$$V_{\min}^{(k)}(s, r) = \min_{s \leq t \leq s+r} V^{(k)}(t),$$

$$V_{\max}^{(k)}(s, r) = \max_{s \leq t \leq s+r} V^{(k)}(t). \quad (6c)$$

Operations (6) normalize each time series in the first adaptation window to the unit peak-to-valley value (formula (6a)), and the normalization in consecutive windows shifted to the right by one sample is only carried out for the endmost term on the right ( $s + r$ ) and

does not affect the previous normalization results (formula (6b)). Variations of the initial time series is thereby adapted to a uniform scale in the window  $r$  samples wide only to the right of the current point. This technique of the *left-oriented adaptation window* will be consistently used below because it is effective for detecting precursor effects, eliminating the “backward” influence of postseismic effects.

Furthermore, let

$$Y_{kj}^{(\alpha)} = Y_k^{(\alpha)}(\tau_j^{(\alpha)}), \quad \alpha = 1, \dots, m; \quad k = 1, \dots, q; \quad (7)$$

$$j = 1, \dots, 2^{(m-\alpha)}; \quad \tau_j^{(\alpha)} = j \times 2^\alpha$$

be the wavelet coefficients in the MRA expansion of the time series  $U^{(k)}(t)$  at an  $\alpha$  detail level.

The wavelet-aggregated signal is constructed in two steps. The first consists in the substitution of the canonical wavelet coefficients for the initial ones (after normalization (6)). Let

$$Q^{(\alpha)}(s, r) = \{Y_{kj}^{(\alpha)} : s \leq \tau_j^{(\alpha)} \leq s + r, k = 1, \dots, q\}, \quad (8)$$

$$j = 1, \dots, L^{(\alpha)}(r)$$

be the set of  $q$ -dimensional vectors whose components are wavelet coefficients, at an  $\alpha$  detail level, in the MRA expansion of the initial multivariate time series for the time indexes  $j$  complying with the condition  $s \leq \tau_j^{(\alpha)} \leq s + r$ . Here,  $s$  and  $r$  are, respectively, the beginning and length of the moving time window of adaptation, expressed in samples. Further,  $L^{(\alpha)}(r)$  is the number of the wavelet coefficients at an  $\alpha$  detail level, for which neighboring time indexes  $j$  fall into the same adaptation window  $r$  samples wide. Because the number of wavelet coefficients decreases with an increase in the order of the detail level as the geometric progression with a ratio of 2,  $L^{(\alpha)}(r)$  decreases at the same rate, and all  $L^{(\alpha)}(r)$  at  $r < N$  may become zero beginning from some  $\alpha$ , i.e., sets (8) will be empty.

Let  $R^{(\alpha)}(s, r)$  be  $q \times q$  matrices that are sample estimates of the covariance matrices of a nonempty set of vectors (8):

$$R^{(\alpha)}(s, r) = \frac{1}{L^{(\alpha)}(r)} \sum_{z \in Q^{(\alpha)}(s, r)} z z^T, \quad (9)$$

where  $z$  are  $q$ -dimensional vectors whose components are the wavelet coefficients at an  $\alpha$  detail level that fall into the time adaptation window  $[s, s + r]$ . When calculating (9), the sample average is not subtracted from the vectors  $z$  because the mathematical expectation of wavelet coefficients is zero. To make estimates (9) statistically significant, I introduce a “representativity threshold”  $L_{\min}$  (an additional parameter of the wavelet-aggregation algorithm), which is a positive integer

number indicating that estimates (9) are only calculated for the  $\alpha$  detail levels satisfying the condition

$$L^{(\alpha)}(r) \geq L_{\min}. \quad (10)$$

It is assumed that the aggregation procedure is inapplicable to the  $\alpha$  detail levels that do not meet condition (10).

I divide the vectors  $z$  into two parts: the scalar  $z_1$  and the  $(q-1)$ -dimensional column-vector  $\xi = (z_2, \dots, z_q)^T$  composed of the remaining components. The scalar product of each vector  $\xi$  by a vector  $\varphi$  specified below yields the set of the scalar quantities  $\zeta_1 = \varphi^T \xi$ . The vector  $\varphi$  is found from the condition that the squared modulus of the correlation coefficient between sets of scalar values  $z_1$  and  $\zeta_1$  is at maximum. This problem is a particular case of the Hotelling classical problem on canonical correlations: the vector  $\varphi$  is found as the eigenvector corresponding to the maximum eigenvalue (equal to the maximum squared modulus of the correlation coefficient between  $z_1$  and  $\zeta_1$ ) of the following  $(q-1) \times (q-1)$  matrix [Hotelling, 1936; Rao, 1968]:

$$S_{\xi\xi}^{-1} S_{\xi z_1} S_{z_1 z_1}^{-1} S_{z_1 \xi}, \quad (11a)$$

$$S_{z_1 z_1} = \text{cov}(z_1, z_1), \quad S_{z_1 \xi} = S_{\xi z_1}^T = \text{cov}(z_1, \xi^T), \quad (11b)$$

$$S_{\xi\xi} = \text{cov}(\xi, \xi^T).$$

Matrices in formulas (11a) and (11b) are obviously submatrices of the general  $q \times q$  covariance matrix  $S_{zz} = \text{cov}(z, z^T)$ . Replacing matrix  $S_{zz}$  in (11) by its sample estimate (9), the vector  $\varphi$  and the set of values of the scalar quantity  $\zeta_1$  can be calculated. I call the  $\zeta_1$  values as canonical wavelet coefficients of the time series  $U_1(t)$  at a given  $\alpha$  detail level in the current adaptation time window  $[s, s+r]$ .

This operation implies that, if the component  $U_1(t)$  at an  $\alpha$  detail level contains a noise characteristic of only this series and is absent from other components (usually caused by anthropogenic factors or systematic errors of measurements), the set of canonical wavelet coefficients is free from such interferences by virtue of its construction. At the same time,  $\zeta_1$  retains all  $\alpha$ -level constituents of the component  $U_1(t)$  which are common to the remaining components of the initial time series (the set of wavelet coefficients  $\xi$ ).

Application of similar operations to the remaining components of the vector  $z$  yields the set of  $q$ -dimensional vectors of canonical wavelet coefficients  $\zeta = (\zeta_1, \dots, \zeta_q)^T$ . For a given length of the adaptation window and detail levels  $\alpha$  satisfying (10), all of the  $L^{(\alpha)}(r)$   $q$ -dimensional vectors  $\zeta$  at  $s=1$  (in the first adaptation window) are stored. Further, displacing the window to the right by one sample, the procedure for the determination of the vector  $\varphi$  is independently performed in each adaptation window; however, rather than the whole cloud of  $q$ -dimensional vectors  $\zeta$  only the vector corresponding to the right end of a given window (i.e.,

to the time  $s+r$ ) is calculated and stored. Canonical wavelet coefficients are thereby adapted to the collective behavior of the multidimensional signal in the previous time window  $r$  samples wide. The adaptation windows are shifted to the right by one sample until the condition  $(s+r) = N$  is met.

As a result, the assemblage of sets of wavelet coefficients (8) at various detail levels is replaced by an analogous assemblage of sets of canonical wavelet coefficients at the detail levels satisfying (10). This concludes the first stage of the wavelet aggregation procedure.

The second stage of this procedure consists in the calculation of the principal component of the canonical wavelet coefficients. Hereinafter, I assume for simplicity that vectors  $z$  in (8) and (9) are composed of canonical, rather than initial wavelet coefficients  $\zeta_{kj}^{(\alpha)}$ . Upon calculating the sample estimate of the covariance matrix of canonical wavelet coefficients at a given detail level  $\alpha$  and in a given adaptation window from a formula similar to (9), the  $q$ -dimensional eigenvector corresponding to the maximum eigenvalue of this matrix is denoted as  $\chi^{(\alpha)}$ . The scalar products of each vector  $\zeta$  by  $\chi^{(\alpha)}$  yields the set of values of the first principal component inherent in the assemblage of vectors  $\zeta$  statistically, this set preserves the maximum information about correlation characteristics of the initial cloud of  $q$ -dimensional vectors [Rao, 1968]:

$$W_j^{(\alpha)} = \sum_{k=1}^q \chi_k^{(\alpha)} \zeta_{kj}^{(\alpha)}. \quad (12)$$

Similar to the first stage, the  $W_j^{(\alpha)}$  values are stored for each  $\alpha$  detail level satisfying (10): the entire set from the first adaptation window at all  $j$  from the interval  $1 \leq j \leq (1+r)$  and only the value corresponding to the right end of each succeeding window,  $j = (s+r)$ . Thus, the  $W_j^{(\alpha)}$  values are determined for all  $\alpha$  satisfying (10) and for all  $j$  from the interval,  $1 \leq j \leq N2^{-\alpha}$ . I set  $W_j^{(\alpha)} = 0$  for those values of  $\alpha$  which do not satisfy (10) and for  $j$  such that  $N \times 2^{-\alpha} < j \leq 2^{(m-\alpha)}$ .

The calculated values of  $W_j^{(\alpha)}$  are considered as the wavelet coefficients of some scalar signal  $W(t)$ , which can be found by means of the fast inverse wavelet transformation and will be referred to as a wavelet-aggregated signal. Thus, a wavelet-aggregated signal is a signal whose wavelet coefficients are principal values of the canonical wavelet coefficients of the initial time series.

It is easy to see that both the first and second stages of the wavelet aggregation consist in a linear transformation applied first to the initial wavelet coefficients in order to obtain the canonical ones and then to the canonical wavelet coefficients in order to transform them to the first principal components. For this reason,

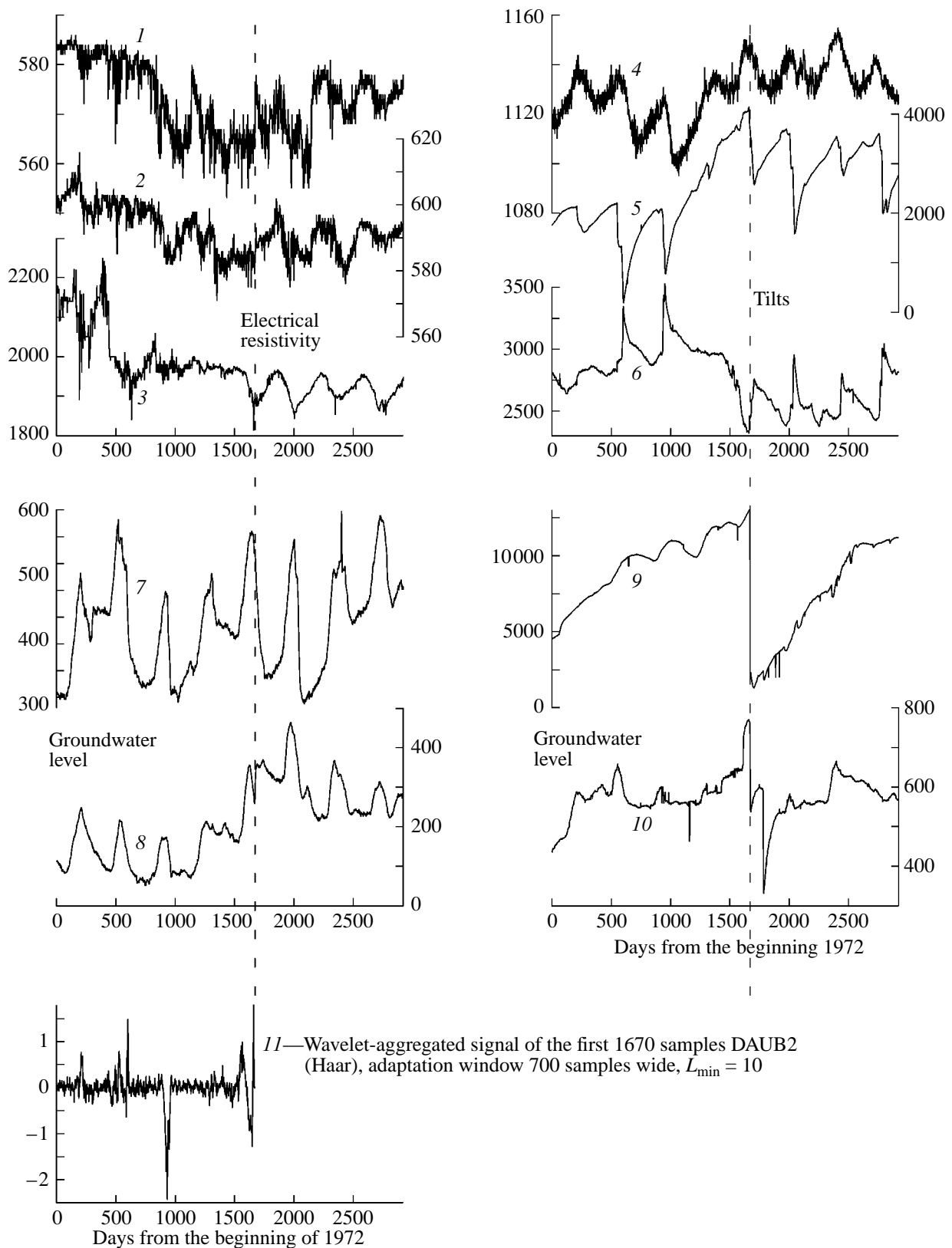


**Fig. 1.** Plots of ten initial time series (1–10) and their wavelet-aggregated signal (11) for the initial 1670 samples (Haar wavelets, adaptation window 700 samples wide,  $L_{\min} = 10$ ). The measurements were made every 24 hours from January 1, 1972 to December 31, 1972. Vertical broken lines mark the moment of the  $M = 7.8$ , Tien Shan earthquake of July 28, 1976 (1671st day from the beginning of 1972).

the aggregation procedure as a whole can be represented as a linear transformation of the initial wavelet coefficients

$$W_j^{(\alpha)} = \sum_{k=1}^q G_{kj}^{(\alpha)} Y_{kj}^{(\alpha)} \quad (13)$$

for  $\alpha$  satisfying (10) with some weights  $G_{kj}^{(\alpha)}$  describing the net effect of the both stage. These weights can be calculated explicitly, but they are not used in the algorithm realization.

Note also that the use of a moving time window in the algorithm described above differs from its use in the spectral approach, in which the Fourier transformation or the evaluation of the covariance function that falls into the sampling window were carried out in each time window independently. In the wavelet analysis, coefficients (7) are calculated for the entire sample, and the moving window is employed for the adaptation to variations in the signal properties when estimating the weights in formula (13).

The description of the algorithm of constructing a wavelet-aggregated signal is completed. Its parameters are

$p$ , the order of an wavelet function (below, only the Daubechies wavelets are used);

$r$ , the width of the adaptation window (measured in samples);

$L_{\min}$ , the representativeness threshold involved in the calculation of sample estimates of covariance matrices.

### A DATA ANALYSIS EXAMPLE

The results derived from the application of the signal aggregation procedure to the combined data from measurements of geophysical parameters in northeastern China are presented in Fig. 1. These data were kindly afforded by Prof. Zhang Zhaocheng from the Center for Analysis and Prediction of Earthquakes, State Seismological Bureau, China. The initial dataset includes ten time series derived from the synchronous recording of the following geophysical parameters:

electrical resistivity of rocks (three series, plots 1 to 3 in Fig. 1);

tilts (three series, plots 4 to 6 in Fig. 1);

variations in the groundwater level in wells (four series, plots 7 to 10 in Fig. 1).

The characteristic linear dimension of the observation network is 200 km. The 8-year interval, from January 1, 1972 to December 31, 1979, was processed. The samples were taken every 24 hours, which provided series consisting of 2922 samples each. The catastrophic Tien Shan earthquake of  $M = 7.8$  occurred on July 28, 1976, i.e., on the 1671st day from the beginning of 1972. This moment is best resolved in plot 9 of

Fig. 1, representing variations in the groundwater level at the point located in the epicentral zone.

The orders  $p = 2, 4,$  and  $12$  were used for the aggregated signal construction (the fast wavelet transform programs for  $p > 2$  were taken from [Press *et al.*, 1996]). From the standpoint of the detection of short-term earthquake precursors, the inferred results were positive in all cases, but the case with  $p = 2$  (Haar wavelet) gave the best results. The latter are presented in Figs. 1 to 3 and are discussed below. The adaptation window width  $r = 700$  samples and the representativeness threshold  $L_{\min} = 10$  were used. The initial 1670 samples or shorter series immediately preceding the moment of the shock were processed.

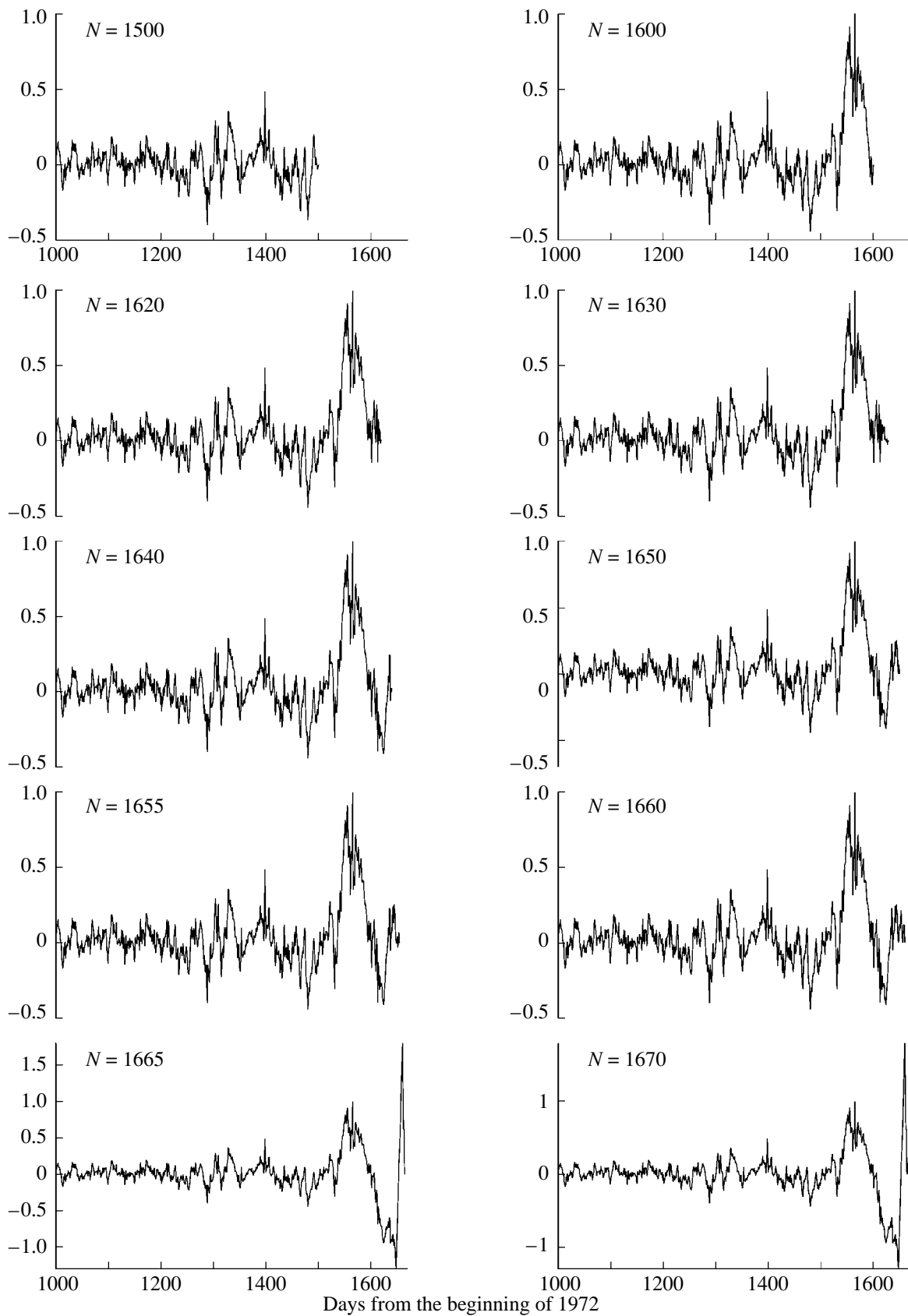
The behavior of the aggregated signal of the first 1670 samples (sample immediately adjacent to the shock moment) recovered from all the ten time series is shown in Fig. 1 (plot 11). It is characterized by an amplitude anomaly preceding the earthquake and beginning 100 days prior to the shock moment. Moreover, plot 11 shows other anomalies within the initial 1000-day interval, which are discussed below.

Figure 2 shows the variation in the aggregated signal pattern in the interval beginning from the 1000th day as a function of an increase in the length  $N$  of the processed sample from 1500 to 1670 samples approaching the shock moment. The most contrasting precursor is seen to have formed five days prior to the earthquake.

Figure 3 illustrates the sensitivity of the precursor to changes in the composition of the processed multivariate time series consisting of the first 1670 samples. Series 9 was first excluded from the processing because of the epicentral position of the related observation point. The behavior of the aggregated signal constructed from the remaining 9 series is presented in Fig. 3 (plot Z-9). Other plots in Fig. 3 represent aggregated signals constructed from nine combinations of eight time series, each combination being derived from the initial set by the elimination of series 9 and one of the remaining series. For example, plot designation Z-9-2 in Fig. 3 means that the aggregate signal is constructed from eight initial time series without series 9 and 2. Examination of these plots shows that the short-term precursor anomaly is present in each of them at the end of the sample processed.

### DISCUSSION AND INFERENCES

A technique is proposed for the construction of a wavelet-aggregated signal detecting those components of variations in a multivariate time series of monitoring systems, which are common to all of the constituent series and may be considered as short-lived anomalies (fluctuations). This technique can be helpful in detecting short-term precursors of strong earthquakes, which was demonstrated by the analysis of data recorded before the Tien Shan, northeastern China earthquake.



**Fig. 2.** Variation in the shape of the right end interval of the wavelet-aggregated signal (Haar wavelet, adaptation window 700 samples wide,  $L_{\min} = 10$ ) as a function of an increase in the length of the processed time interval ( $N$ ) approaching the moment of the earthquake (1671st day).

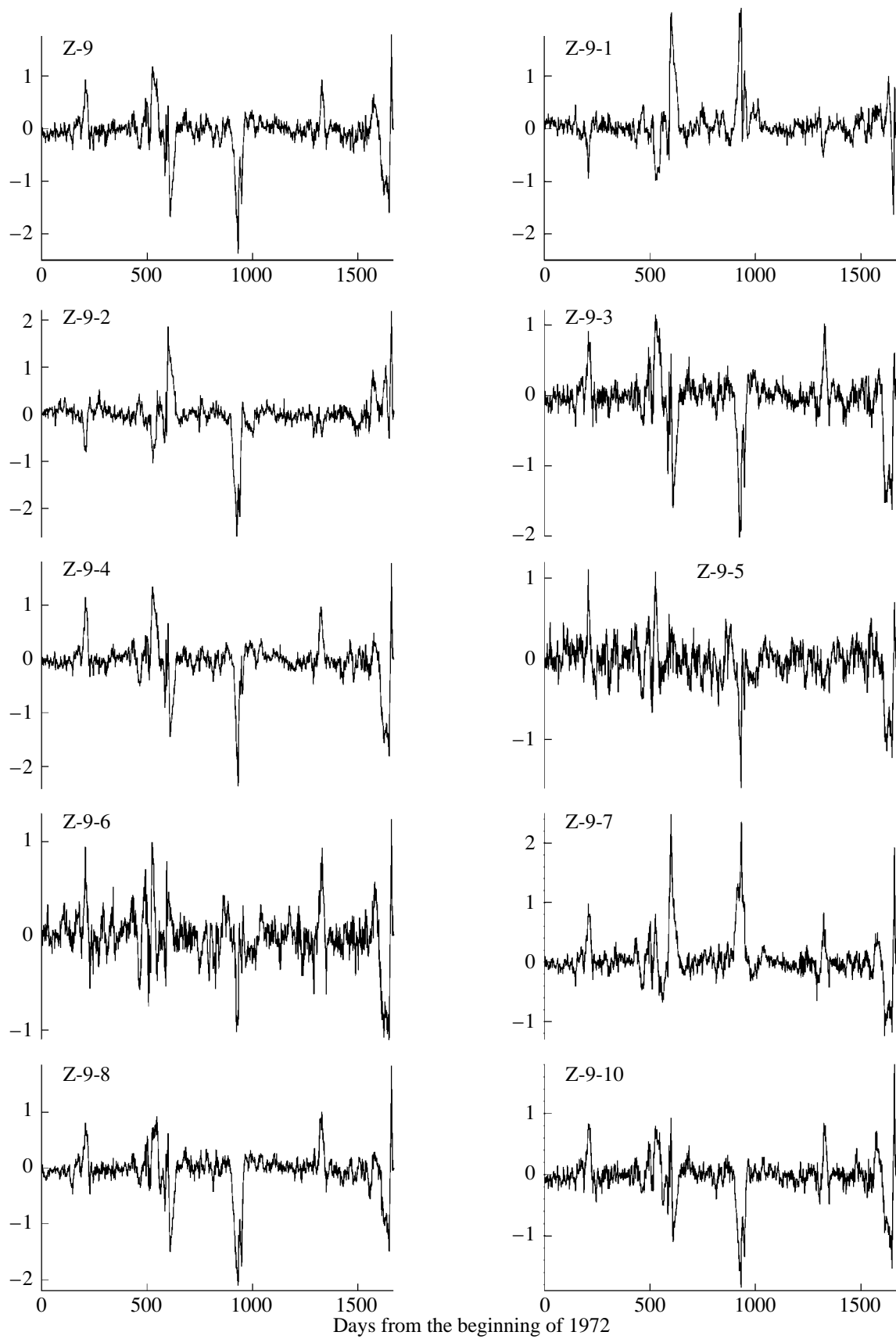
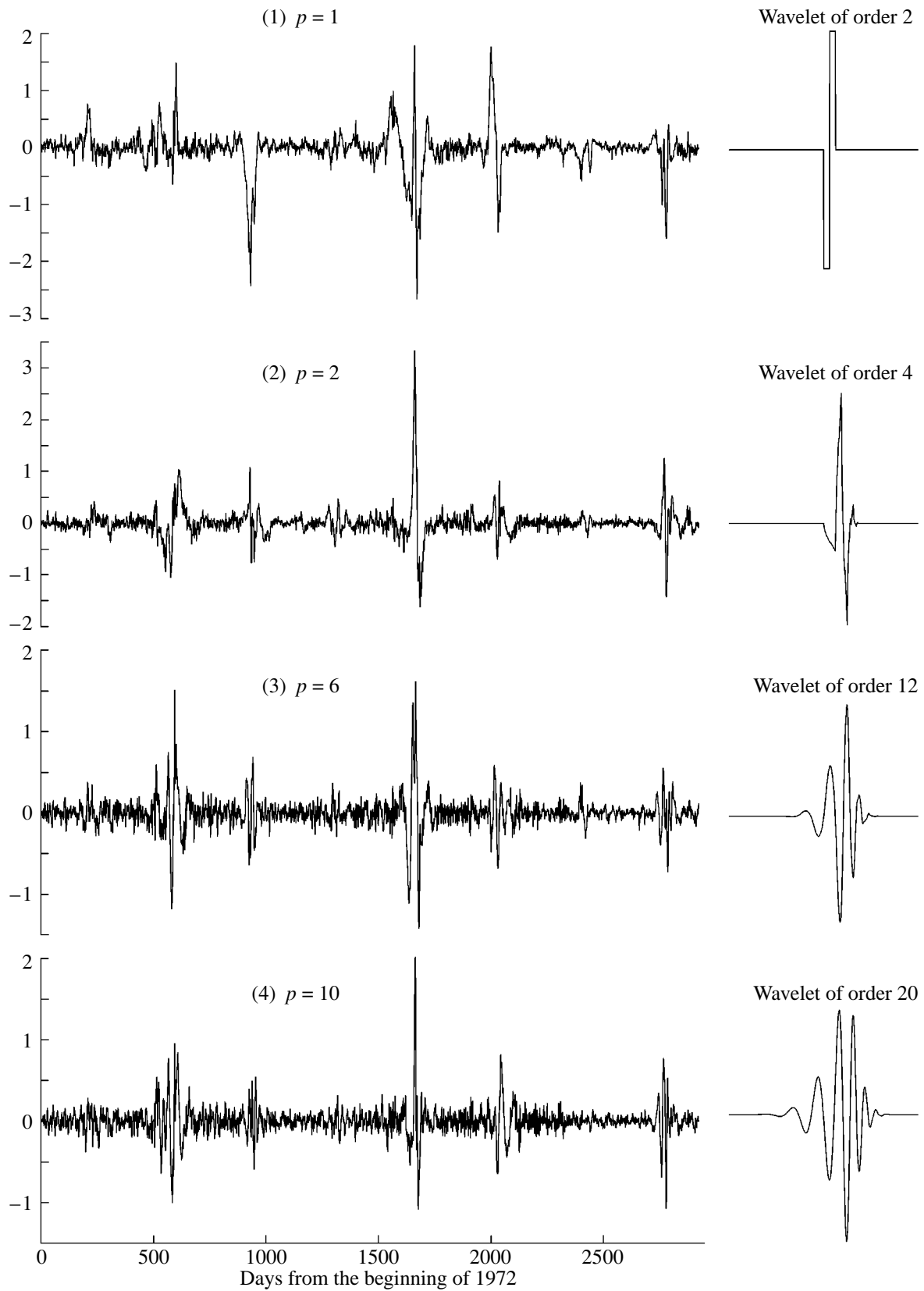


Fig. 3. Various types of wavelet-aggregated signals of the initial 1670 samples.



**Fig. 4.** Wavelet-aggregated signals constructed from the entire time interval by using Daubechies wavelets of various indexes  $p$ . Wavelets of various orders are shown to the right.

The aggregated signals constructed from the entire time interval (from the beginning of 1972 to the end of 1979) with the use of Daubechies wavelets of various orders  $p$  (formula (4)) are shown in Fig. 4. For comparison, the relevant orthogonal wavelets are plotted to the right of the signals. As is seen in all plots, the anomaly associated with the Tien Shan earthquake is the most pronounced. Besides, the figure shows that the use of the Haar wavelets, as compared with the wavelets of higher orders, is advantageous as regards the time of the anomaly formation: in plot (1) of Fig. 4 it appears earlier than in other plots. For this reason, only the results obtained with the use of the Haar wavelets were discussed above.

An anomaly may be roughly considered significant if its amplitude exceeds the level of triple standard deviation. In plot (1) of Fig. 4, this level may be set at approximately 1.0, which gives five significant anomalies (including the Tien Shan anomaly). Other plots presented in Fig. 4 show the presence of the same anomalies.

Apart from the anomaly undoubtedly associated with the Tien Shan catastrophe and considered above, each of the detected significant anomalies is evidence of an increase in the collective constituent of the processes recorded. Here, I do not try to interpret each anomaly as a precursor of a strong event included in the catalog of northeastern China earthquakes. Actually, enhancement of the collective behavior may be caused by a swarm of weak earthquakes or by greater activity of creep movements of the "slow event" type [Lyubushin, *et al.*, 1999]. The above example of the data analysis is an attempt to detect short-term precursors of the Tien Shan earthquake, which confirmed the efficiency of the algorithm proposed in this work.

#### ACKNOWLEDGMENTS

This work was supported by the Russian Foundation for Basic Research, project no. 97-05-64170, and the International Association for the Promotion of Cooperation with Scientists from the Independent States of the Former Soviet Union, grant no. 96-1957.

#### REFERENCES

- Chui, C.K., *An Introduction to Wavelets*, San Diego: Academic, 1992.
- Daubechies, I., Orthonormal Bases of Compactly Supported Wavelets, *Commun. Pure Appl. Math.*, 1988, vol. 41, pp. 909–996.
- Daubechies, I., *Ten Lectures on Wavelets*, CBMS-NSF Series in Applied Mathematics, Philadelphia: SIAM, no. 61, 1992.
- Gilmore, R., *Catastrophe Theory for Scientists and Engineers*, New York: Wiley, 1981. Translated under the title *Prikladnaya teoriya katastrof: v 2-kh knigakh*, Moscow: Mir, 1984.
- Hotelling, H., Relations between Two Sets of Variates, *Biometrika*, 1936, vol. 28, pp. 321–377.
- Kasahara, K., *Earthquake Mechanics*, Cambridge (U.K.): Cambridge Univ. Press, 1981. Translated under the title *Mekhanika zemletryaseni*, Moscow: Mir, 1985.
- Lyubushin, A.A., Jr., Multivariate Analysis of Time Series from Geophysical Monitoring Systems, *Fiz. Zemli*, 1993, no. 3, pp. 103–108.
- Lyubushin, A.A., Jr., Classification of the States of Low-Frequency Geophysical Monitoring Systems, *Fiz. Zemli*, 1994, no. 7, pp. 135–141.
- Lyubushin, A.A., Jr., Analysis of Canonical Coherences in Geophysical Monitoring Problems, *Fiz. Zemli*, 1998a, no. 1, pp. 59–66.
- Lyubushin, A.A., Jr., An Aggregated Signal of Low-Frequency Geophysical Monitoring Systems, *Fiz. Zemli*, 1998b, no. 3, pp. 69–74.
- Lyubushin, A.A., Jr., Kopylova, G.N., and Khatkevich, Yu.M., Spectral Analysis of Hydrogeological Data with Reference to the Seismic Regime in the Petropavlovsk, Kamchatka, Geodynamic Research Area, *Fiz. Zemli*, 1997, no. 6, pp. 79–89.
- Lyubushin, A.A., Jr., Malugin, V.A., and Kazantseva, O.S., Recognition of "Slow Events" in an Aseismic Region, *Fiz. Zemli*, 1999, no. 3, pp. 35–44.
- Nikolis, G. and Prigozhine, I., *Poznanie slozhnogo* (Studying the Complexity), Moscow: Mir, 1990.
- Press, W.H., Flannery, B.P., Teukolsky, S.A., and Vetterling, W.T., *Numerical Recipes*, Chapter 13: Wavelet Transforms, Cambridge: Cambridge Univ. Press, 2nd ed., 1996.
- Rao, S.R., *Lineinye statisticheskie metody i ikh primenenie* (Linear Statistical Methods and Their Application), Moscow: Nauka, 1968.
- Sobolev, G.A., *Osnovy prognoza zemletryaseni* (Fundamentals of Earthquake Prediction), Moscow: Nauka, 1993.